Inorganic Chemistry
Article

Inorg. Chem. **2010**, *49*, 5385–5392 **5385**
DOI: 10.1021/ic902198b

To Bend or Not to Bend: Electronic Structural Analysis of Linear versus Bent M−H−M Interactions in Dinickel Bis(dialkylphosphino)methane Complexes

Zakiya S. Wilson and George G. Stanley*

Department of Chemistry, Louisiana State University, Baton Rouge, Louisiana 70803-1804

David A. Vicic

Department of Chemistry, University of Hawaii, Honolulu, Hawaii 96822-2275

Received November 6, 2009

The M−H−M bonding in the dinuclear complexes $Ni_2(\mu\text{-}H)(\mu\text{-}P_2)_2X_2$ ($P_2 = R_2PCH_2PR_2$, R = *i*Pr, Cy; X = Cl, Br) has been investigated. These dinickel A-frames were studied via density functional theory (DFT) calculations to analyze the factors that influence linear and bent M−H−M bonding. The DFT calculations indicate that the bent geometry is favored electronically, with ligand steric effects driving the formation of the linear M−H−M structures.

Introduction

Linear metal−hydride−metal (M−H−M) structures are rare. Studies on bimetallic complexes with a single bridging hydride have defined this bonding system as "inherently bent".[1−11] While linear M−H−M interactions are rare, X-ray structures of these types have been reported. An early account was suggested by Dahl and co-workers with $[HCr_2(CO)_{10}]^-$.[12,13] According to early crystallographic studies, this bimetallic complex manifested D_{4h} symmetry with eclipsed CO *trans* to the μ-H (top view of Figure 1). While the X-ray structure indicated a very unusual linear μ-H interaction, neutron diffraction studies found the apparent μ-H linearity to result from the disordered average of a crystallographic center of inversion (bottom view of Figure 1).[14,15] Subsequent studies demonstrated that stable linear M−H−M three-center (3C) interactions are rare and pointed to the necessity of neutron diffraction studies for characterizing hydrides, particularly bridging hydrides in transition metal complexes.

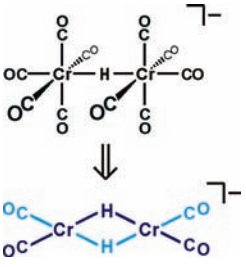

Figure 1. (Top) Initially proposed structure for $[Cr_2(\mu\text{-}H)(CO)_{10}]^-$ derived from crystallographic data. (Bottom) Sketch of the crystallographic center of inversion found by neutron diffraction for the same species. For purposes of clarity, only the CO ligand 180° *trans* to the μ-H is depicted. These studies revealed a Cr−H−Cr angle of 158.9° instead of the 180° suggested by the X-ray structural analysis.

Vicic and co-workers have reported the synthesis and characterization of the most linear Ni−H−Ni interactions in $Ni_2(\mu\text{-}H)Br_2(\mu\text{-dippm})_2$, **1** (dippm = $(i\text{Pr})_2PCH_2P(i\text{Pr})_2$), shown in Figure 2.[16] Neutron diffraction has characterized the M−H−M angle at 177.9° for **1**, with the second largest at 158.9° for $[HCr_2(CO)_{10}]^-$.[14,16,17] **1** is interesting, not only

*To whom correspondence should be addressed. E-mail: gstanley@lsu.edu.

(1) Hart, D. W.; Bau, R.; Koetzle, T. F. *Organometallics* **1985**, *4*, 1590.
(2) Bau, R.; Teller, R. G.; Kirtley, S. W.; Koetzle, T. F. *Acc. Chem. Res.* **1979**, *12*, 176.
(3) Bau, R.; Chiang, M. Y.; Ho, D. M.; Gibbins, S. G.; Emge, T. J.; Koetzle, T. F. *Inorg. Chem.* **1984**, *23*, 2823.
(4) Bau, R.; Koetzle, T. F. *Pure Appl. Chem.* **1978**, *50*, 55.
(5) Bau, R.; Drabnis, M. H. *Inorg. Chim. Acta* **1997**, *259*, 27.
(6) Brown, M. P.; Puddephatt, R. J.; Rashidi, M.; Seddon, K. R. *J. Chem. Soc., Dalton Trans.* **1978**, 516.
(7) Stockland, R. A.; Anderson, G. K.; Rath, N. P. *Inorg. Chim. Acta* **1997**, *259*, 173.
(8) Stockland, R. A.; Anderson, G. K.; Rath, N. P. *J. Am. Chem. Soc.* **1999**, *121*, 7945.
(9) Stockland, R. A.; Anderson, G. K.; Rath, N. P. *Inorg. Chim. Acta* **2000**, *300*, 395.
(10) Teller, R. G.; Bau, R. *Struct. Bonding (Berlin)* **1981**, *44*, 1.
(11) Tenorio, M. J.; Puerta, M. C.; Valerga, P. *J. Chem. Soc., Dalton Trans.* **1996**, 1305.
(12) Handy, L. B.; Treichel, P. M.; Dahl, L. F.; Hayter, R. G. *J. Am. Chem. Soc.* **1966**, *88*, 366.
(13) Handy, L. B.; Ruff, J. K.; Dahl, L. F. *J. Am. Chem. Soc.* **1970**, *92*, 7312.
(14) Roziere, J.; Williams, J. M.; Stewart, R. P.; Petersen, J. L.; Dahl, L. F. *J. Am. Chem. Soc.* **1977**, *99*, 4497.
(15) Petersen, J. L.; Brown, R. K.; Williams, J. M. *Inorg. Chem.* **1981**, *20*, 158.
(16) Vicic, D. A.; Anderson, T. J.; Cowan, J. A.; Schultz, A. J. *J. Am. Chem. Soc.* **2004**, *126*, 8132.
(17) Petersen, J. L.; Johnson, P. L.; O'Connor, J.; Dahl, L. F.; Williams, J. M. *Inorg. Chem.* **1978**, *17*, 3460.

Published on Web 05/25/2010

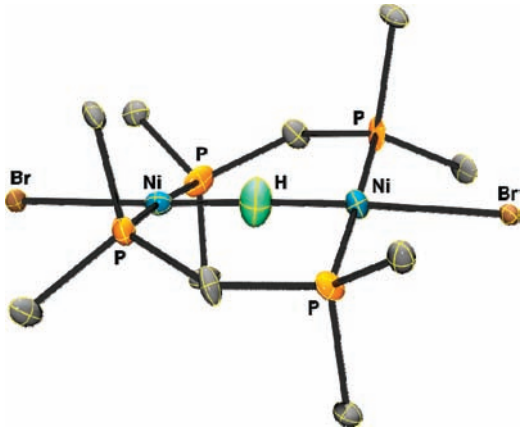

Figure 2. Neutron structure of $Ni_2(\mu\text{-H})Br_2(\mu\text{-dippm})_2$ (**1**).[16] Only the first carbons of the *i*Pr groups are shown for clarity.

because of the near linearity of the μ-H but also because of its structural similarity to A-frames.[18,19] Geometries of this type have been well-characterized and are generally defined as bimetallic complexes with two *trans*-bridging bidentate ligands and at least one other bridging (apex) ligand. Assuming a square-planar coordination about the Ni centers, **1** would likely adopt an A-frame geometry if the Ni−H−Ni interaction were to bend.

Kriley and co-workers have characterized the related complex $Ni_2(\mu\text{-H})Cl_2(\mu\text{-dcpm})_2$, **2** (dcpm = $Cy_2PCH_2PCy_2$), which is isoelectronic with **1**, yet has an A-frame geometry with "inherent" Ni−H−Ni bending (**2** in Figure 3).[20]

The M−H−M linear versus bent structural relationship between **1** and **2** is not new. Several decades ago, Puddephatt and co-workers postulated that A-frames such as $[Pt_2H_2(\mu\text{-H})(dppm)_2]^+$, $[Pt_2Me_2(\mu\text{-H})(dppm)_2]^+$, and $[Pt_2H_2(Cl)(dppm)_2]^+$ manifest fluxionality through geometric inversion and asserted that the only apex ligand small enough to allow this is a bridging hydride (Figure 4).[21]

The most credible experimental evidence for this fluxionality were the ^{1}H NMR chemical signals of the $Ph_2PCH_2PPh_2$ (dppm) methylene bridge protons in $[M_2(\mu\text{-H})X_2(dppm)_2]^+$.[21] In the case of a static structure these give an AB quartet. However, in the case of fluxional inversions only a singlet proton resonance is evident. Through these studies, an energy barrier of 11.106 kcal/mol was estimated for the inversion with the A-frame structure as the lowest energy geometry.[21]

Given the existence of fluxional A-frame inversions, it is not too surprising that stable complexes with linear M−H−M structures have been found. Anderson and co-workers have recently characterized a diamagnetic Pd A-frame, $[Pd_2(\mu\text{-H})R_2(dppm)_2]^+$, whose X-ray-determined crystal structure depicts a linear Pd−H−Pd unit.[8] NMR studies have characterized the methylene bridge of the dppm ligand and found this species inverts in solution.[9]

Both **1** and **2** are paramagnetic with mixed oxidation Ni−Ni states of +1/+2; consequently NMR identification of any solution fluxionality supporting bent−linear interconversions is not possible. Neutron diffraction studies on **1** have been performed, and these have verified that the Ni−H−Ni near linearity is independent of the disordering seen in $[HCr(CO)_{10}]^-$.

Structural studies on both **1** and **2** have been completed by Vicic and co-workers with both Br and Cl ligands.[22] The various structural geometries are shown in Figure 5. External factors such as sterics, hydrogen bonding, and crystal packing forces have been proposed to play an important role in the near linearity of the Ni−H−Ni 3C interaction in the solid-state structure of **1**.[22]

Macchi and co-workers[23] have recently reported electron-density distributions and DFT calculations on $[Cr_2(\mu\text{-H})(CO)_{10}]^-$. They found that the "bent" structure is the most stable, but with low-energy barriers indicating facile fluxionality. The electronic factors affecting linear versus bent μ-H bonding in these A-frame structures, however, has not been studied.[16] It is for this reason that comparative studies of the Ni−H−Ni interactions in **1** and **2** present the opportunity for investigating the stability, electronic, and steric factors influencing the formation of bent and linear structures. Furthermore the nearly linear Ni−H−Ni interaction makes **1** an intriguing model for studying the three-center μ-H molecular orbital interactions in linear M−H−M systems.

Computational Details

Geometries shown in Figure 3 were chosen to gain some insight into the electronic factors affecting the stability of the linear M−H−M interaction. **1** and **2** are the isoelectronic linear and bent nickel complexes discussed earlier. The remaining ones were chosen to represent a variety of halide and phosphine ligand electronic and steric effects.

All geometries symmetrized and using density functional theory as implemented in the Gaussian 98 and 03 systems of programs.[24] Specifically, restricted and restricted open-shell Becke three-parameter Lee−Yang−Perdew (B3LYP) methods[25−27] were used for the diamagnetic and paramagnetic species, respectively. Three sets of calculations were completed with the all-electron basis sets of 6-31G*, 6-31G**, and 6-31G**/6-311G**. After optimization, single-point calculations were completed on all complexes, wherein a Mulliken population analysis was used to study the electronic structure and subsequent bonding present in each species.[28] The AOMix[29,30]

(18) Kubiak, C. P.; Eisenberg, R. *Inorg. Chem.* **1980**, *19*, 2726.
(19) Kubiak, C. P.; Eisenberg, R. *J. Am. Chem. Soc.* **1977**, *99*, 6129.
(20) Kriley, C. E.; Woolley, C. J.; Krepps, M. K.; Popa, E. M.; Fanwick, P. E.; Rothwell, I. P. *Inorg. Chim. Acta* **2000**, *300*, 200.
(21) Puddephatt, R. J.; Azam, K. A.; Hill, R. H.; Brown, M. P.; Nelson, C. D.; Moulding, R. P.; Seddon, K. R.; Grossel, M. C. *J. Am. Chem. Soc.* **1983**, *105*, 5642.
(22) Tyree, W. S.; Vicic, D. A.; Piccoli, P. M. B.; Schultz, A. J. *Inorg. Chem.* **2006**, *45*, 8853.
(23) Macchi, P.; Donghi, D.; Sironi, A. *J. Am. Chem. Soc.* **2005**, *127*, 16494–16504.
(24) Frisch, M. J.; Trucks, G. W.; Schlegel, H. B.; Scuseria, G. E.; Robb, M. A.; Cheeseman, J. R.; Zakrzewski, V. G.; Montgomery, J. A., Jr.; Stratmann, R. E.; Burant, J. C.; Dapprich, S.; Millam, J. M.; Daniels, A. D.; Kudin, K. N.; Strain, M. C.; Farkas, O.; Tomasi, J.; Barone, V.; Cossi, M.; Cammi, R.; Mennucci, B.; Pomelli, C.; Adamo, C.; Clifford, S.; Ochterski, J.; Petersson, G. A.; Ayala, P. Y.; Cui, Q.; Morokuma, K.; Salvador, P.; Dannenberg, J. J.; Malick, D. K.; Rabuck, A. D.; Raghavachari, K.; Foresman, J. B.; Cioslowski, J.; Ortiz, J. V.; Baboul, A. G.; Stefanov, B. B.; Liu, G.; Liashenko, A.; Piskorz, P.; Komaromi, I.; Gomperts, R.; Martin, R. L.; Fox, D. J.; Keith, T.; Al-Laham, M. A.; Peng, C. Y.; Nanayakkara, A.; Challacombe, M.; Gill, P. M. W.; Johnson, B.; Chen, W.; Wong, M. W.; Andres, J. L.; Gonzalez, C.; Head-Gordon, M.; Replogle, E. S.; Pople, J. A.*Gaussian98* and 03, Revision A.11 ed.; Gaussian, Inc.: Pittsburgh, PA, **1998**.
(25) Vosko, S. H.; Wilk, L.; Nusair, M. *Can. J. Phys.* **1980**, *58*, 1200.
(26) Lee, C. T.; Yang, W. T.; Parr, R. G. *Phys. Rev. B* **1988**, *37*, 785.
(27) Miehlich, B.; Savin, A.; Stoll, H.; Preuss, H. *Chem. Phys. Lett.* **1989**, *157*, 200.
(28) Mulliken, R. S. *J. Chem. Phys.* **1955**, *23*, 1833.
(29) Gorelsky, S. I.; Lever, A. B. P. *J. Organomet. Chem.* **2001**, *635*, 187.
(30) Gorelsky, S. I. *AOMix*, Revision 5.61 ed.; http://www.sg-chem.net/aomix/.

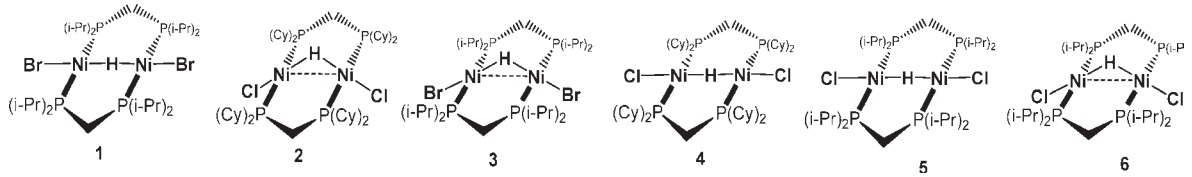

Figure 3. Structures studied via DFT calculations.

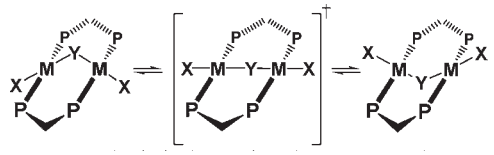

Figure 4. Schematic of a fluxional A-frame inversion with an intermediate containing a linear M−H−M.

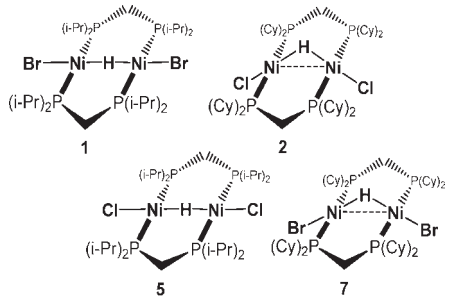

Figure 5. Experimental structures observed for various Ni_2 systems with different bridging phosphine ligands and halides.

system of programs was used to (1) obtain metal and ligand contributions to each molecular orbital (MO) and (2) derive Wiberg and Mayer bond orders via evaluation of the Mulliken population analysis. An analysis of the MO coefficients facilitated the determination of the orbital hybridizations. The MO diagrams of the optimized geometries were generated with Sigma Plot.

Results and Discussion

The focus of this investigation is the stability of the linear versus bent Ni−H−Ni interaction in **1**. Because of its similarity to the bent Ni−H−Ni structure for **2**, we also studied the linear μ-H version of **2**. Notably, the Ni−Ni centers in **1** and **2** are mixed d^8-d^9 configurations, and we expect these NiX_4 systems to adopt square-planar geometries, as evidenced by their solid-state structures.[31] The halides (whether Br or Cl) were, therefore, placed 180° *trans* to the μ-H.[16,20]

Reduced Model Ligands. In *ab initio* and DFT calculations on metal complexes, simplified ligands are often employed to represent larger, more complex ligands. This technique reduces the computational cost while often providing reasonable results. With this in mind, **1** and the A-frame bent analogue **3** were initially studied with simpler $Me_2PCH_2PMe_2$, dmpm, ligands.

Upon optimization with the dmpm ligand, **3-dppm** retained the Ni−H−Ni bending; however, the linear Ni−H−Ni interaction in **1-dppm** underwent bending upon optimization, and the Br ligands migrated from eclipsed positions, relative to the Ni−Ni axis, to a *trans* conformation, with one Br above the Ni−Ni axis and one below this axis (Figure 6).

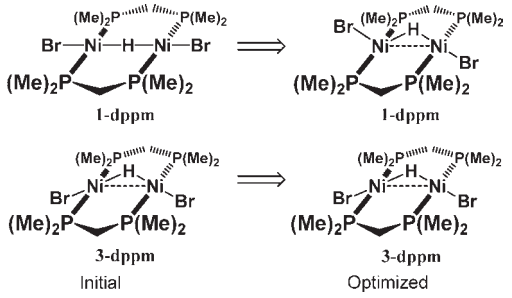

Figure 6. Initial and optimized geometries of **1** and **3** with the dmpm ligand. For **1-dppm**, the linear Ni−H−Ni was unstable and bent; also the Br ligands were migrated from eclipsed positions, relative to the Ni−Ni axis, to a *trans* conformation, with one Br above the Ni−Ni axis and one below this axis. For **3-dppm**, the bent Ni−H−Ni was retained after optimization.

The instability of a linear Ni−H−Ni interaction with the methyl-substituted ligand, dmpm, caused us to consider the larger role of sterics and to a lesser extent the electronic effects via the σ-donor capability of dippm relative to dmpm. Consequently, studies on the linear and A-frame geometries of **1** and **3** with the full dippm ligand were pursued.

Optimized Geometries of the Linear (1) and Bent (3) Structures of $Ni_2(\mu$-H)Br_2(dippm)$_2$. Calculations on two conformational arrangements of $Ni_2(\mu$-H)Br_2(dippm)$_2$ were performed with the linear structure of **1** and its bent A-frame equivalent **3**. Upon geometry optimization, **1** and **3** retained their respective linear and bent Ni−H−Ni structures.

These species, **1** & **3**, were fully optimized under D_2 & C_2 symmetries, respectively, and the molecular energies were computed with three basis sets: 6-31G*, 6-31G**, and mixed-set 6-311G** (with 6-31G** on Ni and Br). For these basis sets a single star indicates that polarization functions were included only on hydrogen atoms. Two stars indicate that polarization functions were added to the remaining atoms. In all cases, structure, **3**, corresponding to the bent M−H−M structure, was the lower energy conformer, and a clear basis set dependence was observed. The smaller 6-31G* calculation showed an energy difference of 36.56 kcal/mol, which is not at all consistent with the experimental work of Puddephatt and co-workers, who found an 11.1 kcal barrier for the bent−linear−bent interconversion.

The 6-31G** set gave a more reasonable energy preference of 3.21 kcal/mol for the bent geometry, indicating the importance of using polarization functions on the heavier atoms. The fact that this system is fairly electron-rich implies more expanded orbitals where the use of polarization functions will play an important role. Notably, this energy corresponded to a restricted-open shell model, where in all electrons in this paramagnetic complex are paired except the one in the highest singly occupied molecular orbital (SOMO).

(31) Cotton, F. A.; Wilkinson, G.; Murillo, C. A.; Bochmann, M. *Advanced Inorganic Chemistry*, 5th ed.; Wiley: New York, 1999.

Table 1. Relative Energy Differences of **1** and **3** and the Chloride Analogues **5** and **6** with dippm Ligands[a]

basis set	species	relative difference (kcal/mol)
6-31G*	**1** (linear)	36.56
ROB3LYP	**3** (bent)	0.00
6-31G**	**1** (linear)	3.21
	3 (bent)	0.00
ROB3LYP	**5** (linear, Cl)	2.17
	6 (bent, Cl)	0.00
6-31G**	**1** (linear)	3.38
UB3LYP	**3** (bent)	0.00
6-31G**/6-311G**	**1** (linear)	3.70
ROB3LYP	**3** (bent)	0.00

[a] Various basis sets were used with either restricted-open or unrestricted spin models.

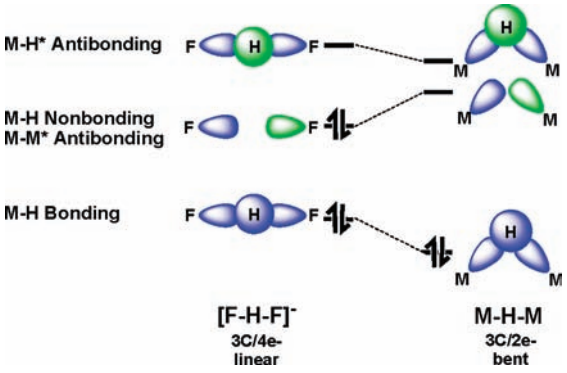

Figure 7. Schematic comparison between the linear and bent X−H−X systems.

Allowing these spins to become fully unpaired using an unrestricted orbital calculation is generally thought to give more accurate energy differences for open shell molecules. Using the 6-31G** basis set the unrestricted calculation gave an energy difference of 3.38 kcal/mol, with the lower energy species again being the bent structure **3**. An additional restricted-open optimization with a combined basis set of 6-31G** (Ni, Br) and 6-311G** (C, H, P) gave an energy difference of 3.70 kcal/mol, with bent **3**, again, as the lower energy structure.

On the basis of the energy differences for all the computed basis sets and spin models, we decided that the 6-31G** restricted-open shell model basis set was accurate enough and computationally reasonable for further studies of the MO interactions in **1** and **3**.

Electronic Structure Analysis and Inspection of the MO Diagrams for 1 and 3. Generally, the MO description for M−H−M bonding is defined in terms of three-center (3C), two-electron (2e) interactions.[32,33] Bau and co-workers presented a classic molecular orbital (MO) explanation for the greater stability of bent M−H−M interactions over their linear analogues (Figure 7).[2] Using a comparative analysis of the M−H−M and F−H−F 3C interactions, he used Walsh diagrams to predict a preference for the M−H nonbonding (M−M σ*) orbital to be unfilled, thereby suggesting a direct relationship between the stability of a bent M−H−M interaction and direct M−M bonding in the 3C interaction. As the $[F-H-F]^-$ nonbonding orbital corresponds to M−M σ* in the M−H−M case, filling the M−M σ* orbital would weaken the M−M bond and by default also weaken the M−H−M 3C interaction. Bau postulated that while this would not be as disadvantageous as filling the M−H* antibonding orbital, it could allow a weakened M−H−M bond to adopt a linear geometry instead of a bent one (i.e., the F−H−F case in Figure 7).

In bimetallic complexes, M−M bonding and overlap are attributed to d-electron availability.[34−36] As bimetallic complexes with mixed oxidation states of d^8-d^9, both **1** and **3** have a substantial number of d electrons, which may destabilize the M−H−M 3C interaction via a filled or partially filled M−M σ*.

Correlated MO diagrams were generated to investigate M−H−M and M−M bonding in both **1** and **3**. Because of our focus on the M−H−M nonbonding (M−M σ*) orbital and its energy difference for both the linear (**1**) and bent (**3**) geometries of $[Ni(dippm)Br]_2(\mu$-H), the most probable pattern for constructing the MO diagram is to correlate the hydride bridge with the $[Ni(dippm)Br]_2$ fragment, henceforth denoted as the <Ni>. A correlated MO diagram of <Ni> with **1** and **3** is presented in Figure 9. (Tables 3 and 4 serve as accompaniments; additional MO diagrams, MO plots, and tables are provided in the Supporting Information.)

Before we go any further in this discussion of M−M and M−H−M bonding, it is necessary to describe the local coordinate system about each Ni center. For both **1** and **3**, the *x*-axis coincides with the Ni−Br bond, the *y*-axis coincides with the Ni−P bond, and the *z*-axis is perpendicular to the Ni−L_4 plane (see the *x*-, *y*-, and *z*-axes labeling in Figure 9).

In **1**, the *z*-axes for both metal centers are parallel. Consequently, we see idealized M(d)−M(d) overlap for **1**, wherein $d_{x^2-y^2}$ corresponds to σ/σ* interactions; d_{xz} and d_{xy} to π/π*; and d_{yz} to δ/δ*. The d_{z^2} is nonbonding and does not interact appreciably with either the ligands or the other metal center. Though M−M overlap patterns are idealized for **1**, the longer M−M distance in this species limits actual M−M orbital overlap, particularly for those orbitals with minimal or low μ-H character.

In **3**, the *z*-axes for both Ni centers are not parallel. In this case, M−M overlap from the d_{yz} orbitals should give δ/δ* bonding but instead gives some π bonding (e.g., MO 197). Additionally, several of the π* orbitals exhibit σ overlap (cf. MOs 191, 193, 195, and 200). MO 196, which should give π overlap, actually depicts σ bonding. These nonideal M−M bonding interactions can best be described as "slipped" π, π*, and δ orbitals; however, for our ensuing discussion, we will describe these in their idealized cases, i.e., π, π*, and δ.[37] Although M−M overlap patterns are not well-defined for **3**, the shorter M−M distance in this species allows greater M−M orbital interactions, both bonding and antibonding, even for those orbitals with low μ-H character. In these cases, the slipped π/π*, δ/δ* MOs also have σ- and π-bonding components.

The MO diagrams for **1** and **3** were correlated to the $[Ni(dippm)Br]_2$, i.e., the <Ni> fragment. For this Ni substructure, the *x*-, *y*-, and *z*-axes are defined most similarly to **3**, wherein the *x*-axis coincides with the Ni−Ni bond,

(32) Wade, K. *Adv. Inorg. Chem. Radiochem.* **1976**, *18*, 1.
(33) Dekock, R. L.; Bosma, W. B. *J. Chem. Educ.* **1988**, *65*, 194.
(34) Cotton, F. A. *Acc. Chem. Res.* **1978**, *11*, 225.
(35) Frenking, G.; Frohlich, N. *Chem. Rev.* **2000**, *100*, 717.
(36) Vahrenkamp, H. *Angew. Chem., Int. Ed. Engl.* **1978**, *17*, 379.
(37) Baik, M. H.; Friesner, R. A.; Parkin, G. *Polyhedron* **2004**, *23*, 2879.

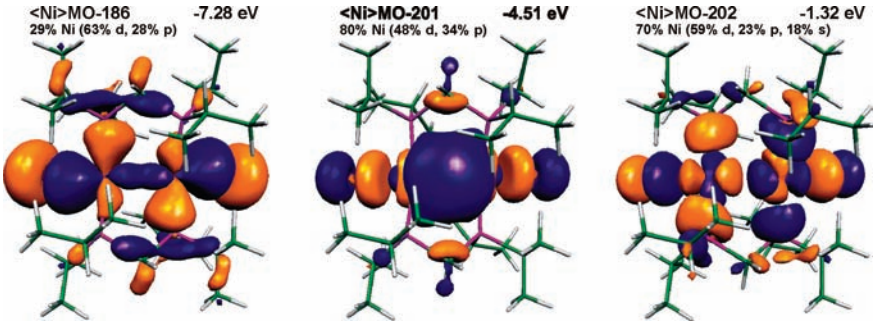

Figure 8. Key molecular orbitals of the $Ni_2(dippm)_2Br_2$ fragment, < Ni >.

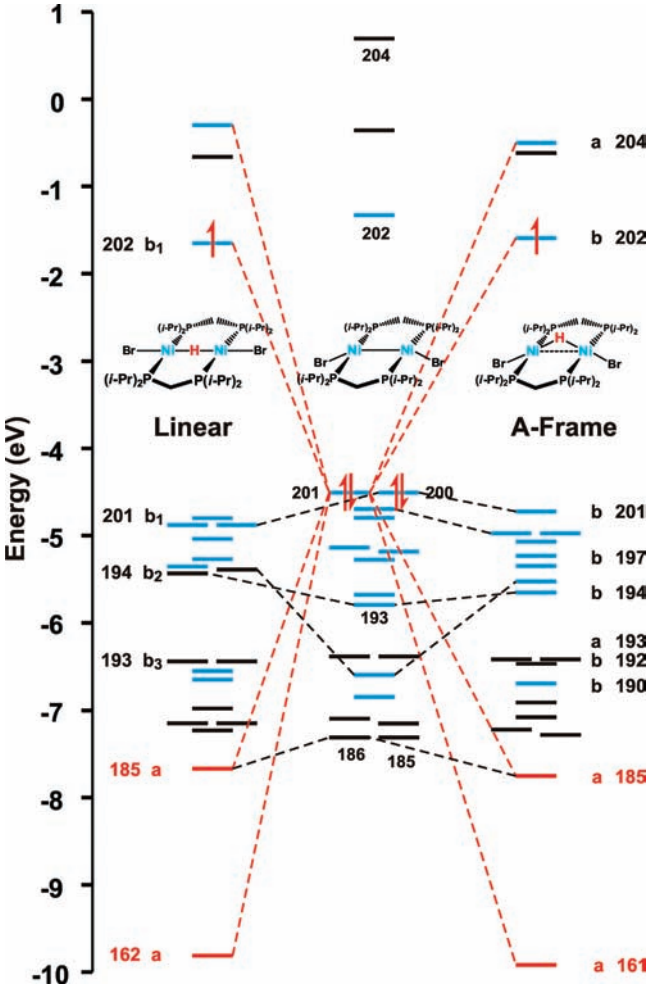

Figure 9. Correlated MO diagram of linear (**1**) and A-frame (**3**) forms of $Ni_2(\mu\text{-H})(dippm)_2Br_2$ with $Ni_2(dippm)_2Br_2$, i.e., < Ni >. All geometries in this diagram were optimized with the B3LYP functional and the 6-31G** basis set. The < Ni > is a neutral spin-paired system, while **1** and **3** are spin-unpaired. The HOMOs are indicated by the electron arrows. MOs with significant Ni character are cyan, while those with hydride character are red.

the *y*-axis coincides with the P—P vector, and the *z*-axis is perpendicular to the Ni_2P_4 plane. In this case, the *z*-axes for both centers are parallel, but we still see examples of "slipped" π/π^* and δ/δ^* overlap.

We are most interested in the primary μ-H orbitals; consequently, two factors are important in analyzing the electronic structure of the Ni fragment. The first is identifying the primary < Ni > orbitals that interact with the μ-H to form the M−H−M 3C bonding, nonbonding, and antibonding combinations. The second is correlating the overall Ni−Ni bonding in the fragment with the Ni−Ni interactions in **1** and **3**.

The lowest metal (d) dominant orbital in the Ni fragment is < Ni > MO-186 (Figure 8). An in-phase combination of two $Ni(d_{x^2-y^2})$−$Ni(d_{x^2-y^2})$ orbitals, this MO depicts a Ni−Ni σ interaction, along with σ bonds with the Br and dippm ligands.

The highest fully occupied molecular orbital (HOMO) is < Ni > MO-201 (Figure 8). It also depicts an in-phase combination of two $Ni(d_{x^2-y^2})$−$Ni(d_{x^2-y^2})$ orbitals, with two additional nodes causing σ^* interactions with the Br ligands. It is nonbonding with the dippm ligands.

The lowest unoccupied molecular orbital (LUMO) is < Ni > MO-202 (Figure 8). It depicts an out-of-phase combination of two $Ni(d_{x^2-y^2})$−$Ni(d_{x^2-y^2})$ orbitals with σ^* interactions with both the Br and dippm ligands.

Of these orbitals, the HOMO (< Ni > MO-201) is particularly important for its interactions with the bridging hydride (μ-H) of **1** and **3**. The in-phase and out-of-phase combinations of < Ni > MO-201 with the μ-H form the critical 3C M−H−M bonding and antibonding interactions depicted in Bau's schematic comparison of linear and bent X−H−X interactions (Figure 7).

Of secondary importance are the intramolecular interactions of < Ni > MO-186 with the μ-H. These also form M−H−M 3C bonding, nonbonding, and antibonding combinations; however in **1** and **3**, these orbitals are low-energy filled orbitals and, as such, do not play as vital a role in examining the relative stability of the Ni−H−Ni interactions in **1** and **3**. In Bau's studies on M−H−M bending, he suggested that significant M−M overlap was a necessary component of the 3C interaction. We have further analyzed the electronic structures of **1** and **3** and have studied both μ-H interactions in the Ni−H−Ni 3C bond and any direct Ni−Ni interactions. Of particular importance is the stability and occupation of the Ni−H−Ni nonbonding (Ni−Ni σ^*) interaction.

The lowest M(d) dominant orbital for the linear **1** and bent **3** geometries of $[Ni(dippm)Br]_2(\mu\text{-H})$ is MO-185 for each structure. In both cases, this orbital results from the in-phase combination of a Ni−Ni σ interaction of < Ni > MO-201 with the μ-H. This forms a classic 3C bond with significant Ni (38%) and H (16%) character. Note that in both cases this orbital has Ni−Br σ^* and Ni−P σ interactions.

The MO study shows that the M−H nonbonding orbital in each system is MO-202 for the linear **1** and bent **3** structures. In both species, this orbital is the highest energy singularly occupied molecular orbital (SOMO).

Table 2. Percent Contribution of Fragments of Selected Orbitals, Based on Mulliken Population Analysis per MO for **1**, D_2 Point Group; RO-B3LYP/6-31G**

			% Ni							
MO	*E* (eV)	sym	total	% s	% p	% d	% H	% Br	% dpm	bonding interactions
204	−0.30	A	55.8	11	21	68	4.2	8.8	31.4	M−H σ *, M−Br σ *, M−P σ *
203	−0.66	B_3	42.0	0	84	15	0.1	2.6	55.4	M−P π
					occupied−unoccupied gap = 0.99 eV					
202	−1.65	B_1	80.2	18	17	65	0.4	8.8	10.6	M−M σ*, M−H nb, M−Br σ*, M−P σ*
201	−4.81	B_1	94.2	44	15	41	0.0	0.5	5.3	M−M nb
200	−4.88	B_2	85.8	0	30	70	0.0	13.6	0.6	M−M π*, M−Br π*
199	−4.89	A	87.3	35	6	60	4.6	0.6	7.5	M−M nb
198	−5.04	B_3	87.6	0	38	62	0.2	12.2	0.2	M−M π*, M−Br π*
197	−5.27	A	89.9	1	1	98	0.0	0.0	10.8	M−M δ*, M−P σ/π
196	−5.36	B_1	87.8	4	4	92	0.0	0.0	13.0	M−M δ, M−P σ/π
195	−5.39	B_3	43.6	0	28	72	0.0	46.8	9.6	M−M π*, M−Br π*, M−P σ
194	−5.41	B_2	33.4	0	35	64	0.0	52.6	14.0	M−M π, M−Br π*, M−P σ
193	−6.44	B_3	14.4	0	50	50	0.0	81.0	4.4	M−Br π
192	−6.44	B_2	16.6	0	47	53	0.0	78.4	4.8	M−Br π
191	−6.55	B_3	49.6	0	25	75	0.0	27.2	23.2	M−M π*, M−Br π, M−P σ
190	−6.64	B_2	54.8	0	35	65	0.2	16.4	28.6	M−M π, M−Br π, M−P σ
189	−6.98	A	13.0	5	55	39	4.2	74.8	8.0	M−H σ*, M−Br σ, M−P σ
188	−7.16	B_1	18.6	23	30	46	0.0	70.0	11.4	M−Br σ, M−P σ
187	−7.17	B_2	12.2	0	63	37	0.0	24.0	63.8	M−Br π, M−P σ
186	−7.22	B_3	9.2	0	86	13	0.0	16.0	74.8	M−Br π, M−P σ
185	−7.67	A	37.8	17	12	71	15.9	0.0	46.3	M−H σ, M−P σ
162	−9.81	A	9.8	54	12	33	18.1	4.8	67.2	M−H σ, M−Br σ, M−P σ

Table 3. Percent Contribution of Fragments of Selected Orbitals, Based on Mulliken Population Analysis per MO for **3**, C_2 Point Group; RO-B3LYP/6-31G**

			% Ni							
MO	*E* (eV)	sym	total	% s	% p	% d	% H	% Br	% dpm	bonding interactions
204	−0.50	A	54.0	7	28	64	5.1	8.6	32.4	M−H σ*, M−Br σ*, M−P σ*
203	−0.62	A	40.4	13	65	21	0.1	3.0	56.6	M-P π
					occupied−unoccupied gap = 0.97 eV					
202	−1.59	B	78.8	12	18	70	0.3	8.8	12.0	M−M σ*, M−H nb, M−Br σ*, M−P σ*
201	−4.72	B	95.4	31	21	48	0.1	4.6	0.2	M−M σ*, M−H nb
200	−4.97	A	94.0	20	20	60	1.0	2.0	3.0	M−M π*, M−Br π*
199	−4.97	B	91.8	43	21	36	0.0	7.0	2.2	M−M δ*, M−P σ
198	−5.07	A	90.0	23	17	60	0.2	6.5	3.3	M−M σ, M−Br π, M−P σ
197	−5.24	B	59.0	10	22	67	0.0	26.0	15.0	M−M δ, M−Br nb, M−P σ*
196	−5.34	A	78.2	16	14	70	1.0	19.6	1.2	M−M π, M−Br π*
195	−5.52	A	63.2	12	24	64	0.3	33.4	3.1	M−M π*, M−Br π*, M−P σ
194	−5.65	B	60.6	4	25	71	0.0	31.0	8.4	M−M π, M−Br π*, M−P σ
193	−6.41	A	28.6	4	33	64	0.0	62.4	9.2	M−Br π, M−P σ
192	−6.42	B	21.0	37	33	30	32.3	75.4	3.6	M−Br π
191	−6.47	A	44.6	8	20	72	0.2	37.2	18.2	M−M π*, M−Br π, M−P σ
190	−6.69	B	57.4	5	19	76	0.2	14.2	28.2	M−M π, M−Br π, M−P σ
189	−6.91	A	12.4	8	51	41	3.9	74.8	9.0	M−H σ*, M−Br σ, M−P σ
188	−7.08	B	20.0	24	33	43	0.0	68.4	11.4	M−Br σ, M−P σ
187	−7.22	A	11.6	1	51	46	0.0	17.4	70.8	M−Br π, M−P σ
186	−7.28	B	12.2	6	52	41	0.0	22.6	65.2	M−Br π, M−P σ
185	−7.75	A	35.0	12	18	70	11.9	0.4	52.8	M−H σ, M−P σ
161	−9.92	A	10.2	47	20	33	17.4	4.8	67.6	M−H σ, M−Br σ, M−P σ

The lowest unoccupied molecular orbitals (LUMO) of **1** and **3** both depict Ni−P π back-bonding through the Ni (p_z) interactions with the dippm π* system. For this orbital (MO-203), we see significant Ni (40−45%) and dippm (55−60%) character.

The pronounced similarity in SOMO energies for the Ni−Ni σ* orbital in the linear and bent geometries is puzzling. One would expect that any reduction in Ni−Ni σ* overlap would lower its energy, such that this orbital should be higher in energy for **3** and lower in energy for **1**, and in fact the SOMO is slightly higher in energy for **3**, but only by 0.06 eV.[38] Considering the differences in Ni−Ni distances of 3.216 Å for **1** and 2.709 Å for **3**, one would expect a considerably stronger Ni−Ni orbital interaction in **3**, which should cause a larger energy difference for the M−M σ* SOMO (MO-202) in **1** and **3**. But the energies of −1.65 and −1.59 eV are very close, so there seems to be little difference in partially filling these two M−M σ* orbitals.

A more careful inspection of the metal−metal bonding can shed some light on the relative stabilities of the M−H nonbonding (M−M σ*) SOMO in **1** and **3**.[37] We have assumed that filling or partially filling the M−M σ* SOMO will destabilize the M−M interaction. The destabilization of X−X interactions in a linear X−H−X system may be true in $F-H-F^-$, but the more complex

(38) Hoffman, D. M.; Hoffmann, R. *Inorg. Chem.* **1981**, *20*, 3543.

Table 4. Calculated Bond Distances and Mayer Bond Indices for Ni−Ni and Ni−L Interactions in the < Ni > Fragment, **1** and **3**

species	bond type	bond distance	Mayer index Lowdin basis		spin-inclusive Mayer index, M^s	
< Ni >	Ni−Ni	2.438	1.052		N/A	
	Ni−Br	2.438	0.981			
	Ni−P (dippm)	2.207	1.443			
			1.505			
1	Ni−H	1.608	0.420	(0.304)	0.024	(−0.038)
	Ni−Ni	3.216	0.480	(0.456)	0.406	(0.384)
	Ni−Br	2.420	1.020	(1.024)	0.782	(0.802)
	Ni−P (dippm)	2.223	1.413	(1.420)	0.901	(0.899)
2	Ni−Ni	2.723	0.650		0.180	
	Ni−H	1.572	0.497		0.409	
	Ni−Cl	2.345	0.827		0.721	
	Ni−P (dcpm)	2.235	1.379		0.894	
			1.456			
3	Ni−Ni	2.709	0.638	(0.556)	0.155	(0.085)
	Ni−H	1.580	0.492	(0.484)	0.405	(0.398)
	Ni−Br	2.441	1.002	(0.992)	0.911	(0.901)
	Ni−P (dippm)	2.234	1.355	(1.340)	0.856	(0.881)

bimetallic systems often have M−M interactions that do not involve the bridging ligand.[37] This means that filling (or partially filling) the M−H nonbonding MO (M−M σ^*) may not, in and of itself, cause a net destabilization of the M−M interaction.

In order to probe this effect more closely, we have extended our investigation of the net Ni−Ni bonding in **1** and **3** in order to gauge the variance of Ni−Ni interactions on the net stabilization of these complexes.

Bond Order and Overlap in 1 and 3. In Bau's studies on M−H−M bending, he suggested that significant M−M overlap was a necessary component of the 3C interaction.[2,4] Accordingly, it is important to investigate the overall Ni−Ni interactions in **1** and **3** in order to gauge the Ni−Ni bond strength. While the longer Ni−Ni distance of 3.216 Å in **1** as compared to 2.709 Å in **3** does suggest stronger Ni−Ni orbital interactions in the bent geometry, the relationship between M−M bond distance and bond order is not always that simple.[39] In fact, studies have shown that the steric and electronic properties of bridging ligands can influence M−M distances by extending and contracting the interactions from what would normally occur in the absence of the bridge(s).[34,36,39] In fact, Baik and co-workers have discussed the dramatic variance of M−M bond distances and bond order for several bimetallic Mo complexes.[37,40−44] Consequently, the shorter M−M bond distance in **3** does not necessarily indicate increased M−M bonding or overlap.

To this end, we have computed Mayer (M) bond indices for the Ni−Ni, Ni−H, Ni−P, and Ni−Br interactions in **1** and **3**.[35,45−51] Although bond orders are not true quantum mechanical observables, they can provide quantitative evaluations of intramolecular interactions.[35] In recent years, Mayer bond indices have gained popularity as a means for investigating bonding and orbital overlap in transition metal complexes, and these have been found to be particularly useful for evaluating M−M bonding when bridging ligands are present.[37,45,52]

For the Mayer bond order analysis, seven subgroups were defined: the two Ni centers, the two Br ligands, the hydride bridge, and two dippm ligands. The Mayer analyses were completed for the restricted open-shell and unrestricted shell B3LYP functionals with the 6-31G** set.

For these indices, any value below 0.300 indicates a nonbonding interaction. Overall, the regular Mayer indices give stronger M−M and M−L interactions than the spin-dependent indices. It is our opinion that the spin-inclusive Mayer index is best for evaluating the bonding in the paramagnetic complexes of **1** and **3**.

For the < Ni > fragment, the Mayer indices indicate a single bond for the Ni−Ni and Ni−Br interactions and 11/2 bond order for Ni−P. For **1** and **3**, the Mayer indices indicate a nonbonding interaction between the two nickel centers, a half (1/2) bond for Ni−H giving rise to the Ni−H−Ni 3C interaction, and single bonds for Ni−Br and Ni−P.

A-Frame Fluxionality and the Linear Ni−H−Ni in 1. The nonbonding nature of the Ni−Ni interaction provides an additional insight into the role of direct Ni−Ni bonding in stabilizing the linear Ni−H−Ni in **1**. In the molecular orbital discussion of **1** and **3**, we found that partially filling the M−H−M nonbonding (M−M σ^*) orbital does not significantly affect the stability of the M−H−M 3C interaction, and the Mayer indices indicate a lack of direct Ni−Ni interactions in both **1** and **3**. These two factors support the idea of A-frame fluxionality as a prevalent role in facilitating the linear Ni−H−Ni geometry of **1** in the solid state.

As we have previously stated, A-frame inversions are not uncommon. In fact, for hydride-bridged A-frame complexes, this fluxionality has produced linear M−H−M systems that exist in the solid state (e.g., the Pd−H−Pd species characterized by Kriley and co-workers[20]). In the case of **1** and **3**, the lack of direct Ni−Ni interactions favors the fluxional behavior of inverting A-frames. If strong Ni−Ni interactions were present in the bent (A-frame) geometry of **3**, Ni−Ni bond breaking would be required for transitioning to the linear geometry, and this would require a considerably higher input of energy. As direct Ni−Ni bonding is minimal in **3**, the fluxional behavior that we have proposed for **1** and **3** does seem favorable.

Conclusions. The linearity of the Ni−H−Ni interaction in [Ni(μ-dippm)Br]$_2$(μ-H) (**1**) has been studied by DFT calculations. This species is proposed to bear a close structural relationship to A-frames. Comparing **1** with an isoelectronic species, **2**, it was found that crystal packing plays a role in disallowing Br bending from the Ni−Ni

(39) Cotton, F. A.; Walton, R. A. *Multiple Bonds between Metal Atoms*, 2nd ed.; Clarendon Press: Oxford, 1993.
(40) Connelly, N. G.; Dahl, L. F. *J. Am. Chem. Soc.* **1970**, *92*, 7470.
(41) Grebenik, P. D.; Green, M. L. H.; Izquierdo, A.; Mtetwa, V. S. B.; Prout, K. *J. Chem. Soc., Dalton Trans.* **1987**, 9.
(42) Green, J. C.; Green, M. L. H.; Mountford, P.; Parkington, M. J. *J. Chem. Soc., Dalton Trans.* **1990**, 3407.
(43) Shin, J. H.; Parkin, G. *Polyhedron* **1994**, *13*, 1489.
(44) Chisholm, M. H.; Cotton, F. A.; Extine, M. W.; Kelly, R. L. *J. Am. Chem. Soc.* **1979**, *101*, 7645.
(45) Bridgeman, A. J.; Cavigliasso, G.; Ireland, L. R.; Rothery, J. *J. Chem. Soc., Dalton Trans.* **2001**, 2095.
(46) Ponec, R.; Mayer, I. *J. Phys. Chem. A* **1997**, *101*, 1738.
(47) Bridgeman, A. J.; Cavigliasso, G. *Faraday Discuss.* **2003**, *124*, 239.
(48) Mayer, I. *Chem. Phys. Lett.* **1983**, *97*, 270.
(49) Mayer, I. *J. Mol. Struct. (THEOCHEM)* **1992**, *87*, 1.
(50) Mayer, I. *Theor. Chim. Acta* **1991**, *79*, 377.
(51) Mayer, I. *Int. J. Quantum Chem.* **1984**, *26*, 151.
(52) Jiang, X.; Bollinger, J. C.; Baik, M. H.; Lee, D. *Chem. Commun.* **2005**, 1043.

axis, thus supporting the linearity of the Ni−H−Ni interaction in the solid state.

Correlated MO diagrams for **1** and its A-frame equivalent, **3**, were made. Noting the role of Bau's qualitative explanation for M−H−M bending, we found that the electronic structures of **1** and **3** both gave M−H nonbonding orbitals that were partially filled. The similarity of these MO energies leads us to propose that the partial filling of the Ni−Ni σ^* orbital does not significantly affect the stabilization of the Ni−H−Ni interaction in **1** and **3**.

The investigation of the net Ni−Ni bonding in **1** and **3** demonstrates minimal direct Ni−Ni interactions in either complex. The lack of direct or significant Ni−Ni bonding further supports the proposed fluxional behavior of **3** with **1** as a linear intermediate that is frozen out in the solid state.

Acknowledgment. This research was supported by NSF (CHE-01-11117, GGS) and DOE (DEFG02-07ER-15885, DAV) and dedicated to Robert Bau, who passed away on December 28, 2008. This research was conducted with high performance computational resources provided by Louisiana State University (http://www.hpc.lsu.edu).

Supporting Information Available: Details of the DFT calculations including molecular orbital plots, optimized coordinates, distances, and angles. This material is available free of charge via the Internet at http://pubs.acs.org.